SEMARAK ILMU PUBLISHING

Journal of Advanced Research in Fluid Mechanics and Thermal Sciences

Journal homepage:
https://semarakilmu.com.my/journals/index.php/fluid_mechanics_thermal_sciences/index
ISSN: 2289-7879

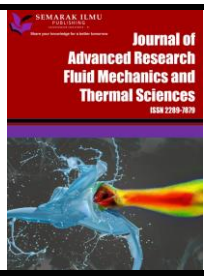

Experimental Investigation on the Aerodynamic Parameters of Trailing Edge Wake Generators

Mohamed Ibren[1], Waqar Asrar[1,*], Muhammad Ariffuddin Ismail[1], Amelda Dianne Andan[1]

[1] Department of Mechanical and Aerospace Engineering, Faculty of Engineering, International Islamic University Malaysia, 53100, Kuala Lumpur, Malaysia

ARTICLE INFO

Article history:
Received 20 October 2023
Received in revised form 6 March 2024
Accepted 17 March 2024
Available online 15 April 2024

Keywords:
Aerodynamic parameters; NACA 0015 airfoil; low Reynolds number; experimental

ABSTRACT

In the realm of aerodynamics, the investigation of airfoil performance stands as a critical domain, with an ever-growing emphasis on optimizing designs for enhanced efficiency. This study investigates the aerodynamic performance of a NACA 0015 airfoil featuring various trailing edges, including serration, comb, poro-serration, and comb-serration. The experiments were conducted in a wind tunnel at angles of attack ranging from -15° to 15° and Reynolds numbers of 1.5 x 10^5 and 2.0 x 10^5. To accurately quantify the forces and moments acting on the airfoil models, a calibrated six-component balance was utilized to measure the aerodynamic coefficients of each airfoil configuration. The lift coefficient (c_l), drag coefficient (c_d), and pitching moment coefficient (c_m) are analyzed for the various trailing edge types and Reynolds numbers. Results indicate that the baseline model demonstrated better aerodynamic performance compared to other types of trailing edge. Most trailing edges, except the baseline, resulted in a decrease in the lift coefficient. However, at very low angles of attack, the airfoil showed an improvement in the maximum lift coefficient. Most trailing edges exhibited an increase in the drag coefficient at a Reynolds number of 1.5 x 10^5. However, at a Reynolds number of 2.0 x 10^5, the drag coefficient showed a similar trend as the baseline. All types of trailing edges, including the baseline, displayed a similar trend in the pitching moment coefficient. When evaluating the lift coefficient to drag coefficient ratio, all trailing edges generally performed similarly at all Reynolds numbers. In general, the baseline model emerges as the optimal choice, showcasing superior aerodynamic characteristics across the evaluated parameters.

1. Introduction

It is important to know the flow structure as well as the laminar boundary layer instability that is present in the flow over an airfoil. The flow over airfoils at low Reynolds numbers ($1 \times 10^4 \leq Re \leq 2 \times 10^6$) is not the same as the flow over airfoils at higher Reynolds numbers. At a low Reynolds number, the TS waves that propagate within the laminar boundary get amplified in the separated shear layer as the unfavorable pressure gradient builds up on the surface of the airfoil [1]. After separating from the airfoil surface, the laminar boundary layer quickly transforms into turbulent flow by forming

* *Corresponding author.*
E-mail address: waqar@iium.edu.my

https://doi.org/10.37934/arfmts.116.1.116

unstable vortex formations [2]. The separated flow then reattached itself as the turbulent flow produced enough unfavorable pressure gradient, resulting in the formation of a laminar separation bubble on the surface of the airfoil.

Flow separation and the formation of laminar separation bubbles have significant implications on the flow topology of airfoils that are operating at lower Reynolds numbers. When the Reynolds number is lower, the separated laminar boundary layer transitions to turbulent flow very quickly by forming an unstable vortex structure, and this is often followed by flow reattachment [3]. As a result, bubbles of laminar separation are created. Additionally, the size of the laminar separation bubble is not only determined by the Reynolds number but also by the angle of attack [4]. When the Reynolds number and angle of attack are increased, the size and position of the separation bubble shift, which results in a change in the structure of the fluid flow over a body [5]. When the angle of attack is relatively low, laminar separation bubbles have the potential to develop on either side of the airfoil. When the angle of attack is increased, there is a corresponding reduction in the boundary layer separation, which in turn causes a reduction in the size and extent of the laminar bubble separation on the airfoil pressure side [6]. Laminar separation bubbles will make the boundary layer thicken and can affect the aerodynamic performance. Hence, it can cause the drag coefficient to increase while the lift coefficient decreases. The aerodynamic performance can be negatively affected by the separation and consequently stalling at a low Reynolds number.

Many investigations have demonstrated that airfoil aerodynamic performance is highly delicate to flow conditions at low Reynolds numbers. In particular, the lift coefficient, separation point, and stalling are all extremely sensitive to even small changes in airfoil design [7]. For a given angle of attack, where the lift force is large, the drag force is relatively low [8]. After that point, the ratio of lift to drag starts to swing in the opposite direction due to flow separation. At a Reynolds number of approximately 3×10^6, it has been observed that the lift coefficient increases up to a specific angle of attack, known as the stall angle [8]. Beyond this angle, the lift coefficient decreases due to stall, a phenomenon resulting from flow separation when the velocity becomes too low and detaches from the airfoil surface. Additionally, the angle of attack influences the drag coefficient, demonstrating that an increase in the angle of attack corresponds to an increase in the drag coefficient.

The flow measurements indicate a reduction in flow acceleration over the porous trailing edges, leading to a delayed and weaker vortex shedding compared to blunt edges. Research findings show that lift decreases and drag increases for the porous section, with lift values decreasing and drag values increasing as flow resistivity rises. Experimentally determined lift, drag, and moment coefficients exhibit significant variations with porosity. Specifically, the lift coefficient decreases with increasing porosity, and drag generally increases with higher porosity. It's worth noting that the increased drag coefficient may result from the flow through the porous region, leading to a rise in viscous drag. Overall, the observed trend is that as porosity increases, the lift coefficient decreases, and drag tends to increase [9]. However, at very low angles of attack, the porous wing outperforms the solid wing in terms of the lift coefficient. In contrast, both solid and porous wings exhibit a similar trend for the drag coefficient [9]. Another study found no significant difference in the poro-serrated model when compared to the baseline. However, at higher angles of attack, both poro-serrated trailing edges, with smaller and larger gaps in each serration, exhibit a reduction in lift coefficient compared to the baseline and continue to perform poorly in the post-stall environment [10]. Similarly, the drag coefficient for all three types follows a similar trend at very low angles of attack. Nevertheless, at a 10° angle of attack, both poro-serrated trailing edges with smaller and larger gaps in each serration demonstrate a reduction in drag coefficient compared to the baseline, and this reduction persists until higher angles of attack [10].

Another aerodynamic concept involves serrations, strategically designed to split the airflow as it traverses them. This division results in a deceleration of the airflow and an increase in pressure at the airfoil's maximum thickness point when subjected to an angle of attack [11]. The presence of eddies and vortices in the separated flow leads to an increase in drag and a decrease in lift when an unstable pattern emerges [12]. Enhancing the flat back airfoil's trailing edge by rounding it has been shown to improve the lift-to-drag ratio and effectively manage flow separation [13]. Additionally, a serrated trailing edge causes the separation point to move closer to the trailing edge [11]. The extension and serration of the trailing edge significantly impact wing aerodynamics, primarily due to adjustments and modifications made to the airfoil's camber and the flow pattern at the trailing edge [14]. The conventional wing is associated with separated flow and a thick wake, while the wing featuring an extended trailing edge promotes attached flow and a thin wake. On the other hand, the wing with a serrated trailing edge is designed for controlled flow separation [11]. Serrated versions with a longer base length exhibit improved stall characteristics, including a delayed stall angle and a smoother stall, while maintaining the same lift coefficient. Conversely, the serrated edge with a shorter base length (2 cm) and an aspect ratio of 1 demonstrates a significant increase in both lift coefficient and a smoother stall. Furthermore, the airfoil model with the extended and serrated trailing edge experiences a higher drag coefficient compared to the baseline model [11].

The extended and serrated edges serve as an effective flow control mechanism, transforming the hard stall (experienced at the leading edge) into a smooth stall (experienced at the trailing edge) within the specified range of angle of attack and free stream velocity [15]. While the investigation of aeroacoustics and sound was the primary focus in studying combed and combed-serrated trailing edges, there has been limited research on the aerodynamic parameters of airfoils with these trailing edges. Given this knowledge gap, the current research aims to explore the impact of combed-serrated trailing edges on the aerodynamic efficiency of this type of configuration.

2. Methodology

2.1 Experimental Setup

In this study, experiments were conducted within the low-speed open circuit - wind tunnel at IIUM, depicted in Figure 1. The wind tunnel's operational range extended to a maximum airspeed of 35 m/s, with experimentation carried out at free-stream velocities of 10 m/s, 15 m/s, and 20 m/s. The chosen NACA 0015 airfoil served as the experimental model, and Reynolds numbers were computed based on the analysis of the airfoil's chord and free-stream flow parameters. The angle of attack, ranging from -15° to 15°, was precisely controlled in 1-degree increments using software inputs. The test section, measuring 300 x 300 mm, incorporated a six-component balance for comprehensive force and moment measurements. To facilitate observation, a window was integrated into the test section to monitor the model's positioning relative to the airflow. Moreover, a contraction section in the upstream portion, equipped with honeycomb-like screens, eliminated turbulent airflow. The airfoil was attached to the wind tunnel turntable via its root, and a Pitot-static tube measured the stagnation and static pressures.

For the fabrication of the mounting plate and airfoil connector, Aluminum 6061, mirroring the airfoil material, was employed. The raw materials underwent a meticulous fabrication process, involving surface grinding and CNC milling to create the requisite screw holes, ensuring precise fitting onto the calibrated six-component balance.

Data acquisition was performed through the utilization of the Data Acquisition Reduction and Control System (DARCS) software. Before introducing airflow to the test section, the force balance underwent calibration. Initial force readings were acquired with the wind tunnel fan inactive due to

a recognized error in the calibrated six-component balance. On top of that, several readings also had been taken while doing the testing because there were many limitations on the calibrated six-component balance. Each angle of attack was subjected to three force measurements. Subsequently, the wind tunnel fan was activated, and the height difference recorded by the manometer determined the flow speed and hence the Reynolds number.

Throughout testing, notable disturbances manifested as vibrations or stall conditions, were observed, particularly after reaching maximum lift coefficients at 12 and 15 degrees of angle of attack. These vibrational phenomena significantly influenced the accuracy of the recorded data. Moreover, at higher angles of attack, the airfoil's flow exhibited increased unsteadiness due to heightened separation, flow separation, or vortex shedding, introducing vibrations that affected the structural integrity and subsequent measurements.

Fig. 1. IIUM low-speed wind tunnel

2.2 Airfoil Model Preparation

The present study focuses on the investigation of the aerodynamic parameters of trailing edge wake generators of a NACA 0015 airfoil with a chord length of 0.15 m and span length of 0.298m, as depicted in Figure 2. In addition to analyzing the baseline NACA 0015 airfoil, this study explores alternative trailing edge configurations, as illustrated in Figure 3 to Figure 6. These configurations include serrated, comb, comb-serrated, and poro-serrated designs. Serrations on the airfoil's trailing edge denote the presence of small triangular or sawtooth-shaped notches. The combed trailing edge entails the integration of small comb-like structures along the trailing edge. Meanwhile, the comb-serration trailing edge combines both comb-like structures and serrations. The poro-serration trailing edge introduces a series of small openings within the serration along the trailing edge. The specifications of the modified trailing edge are as follows:

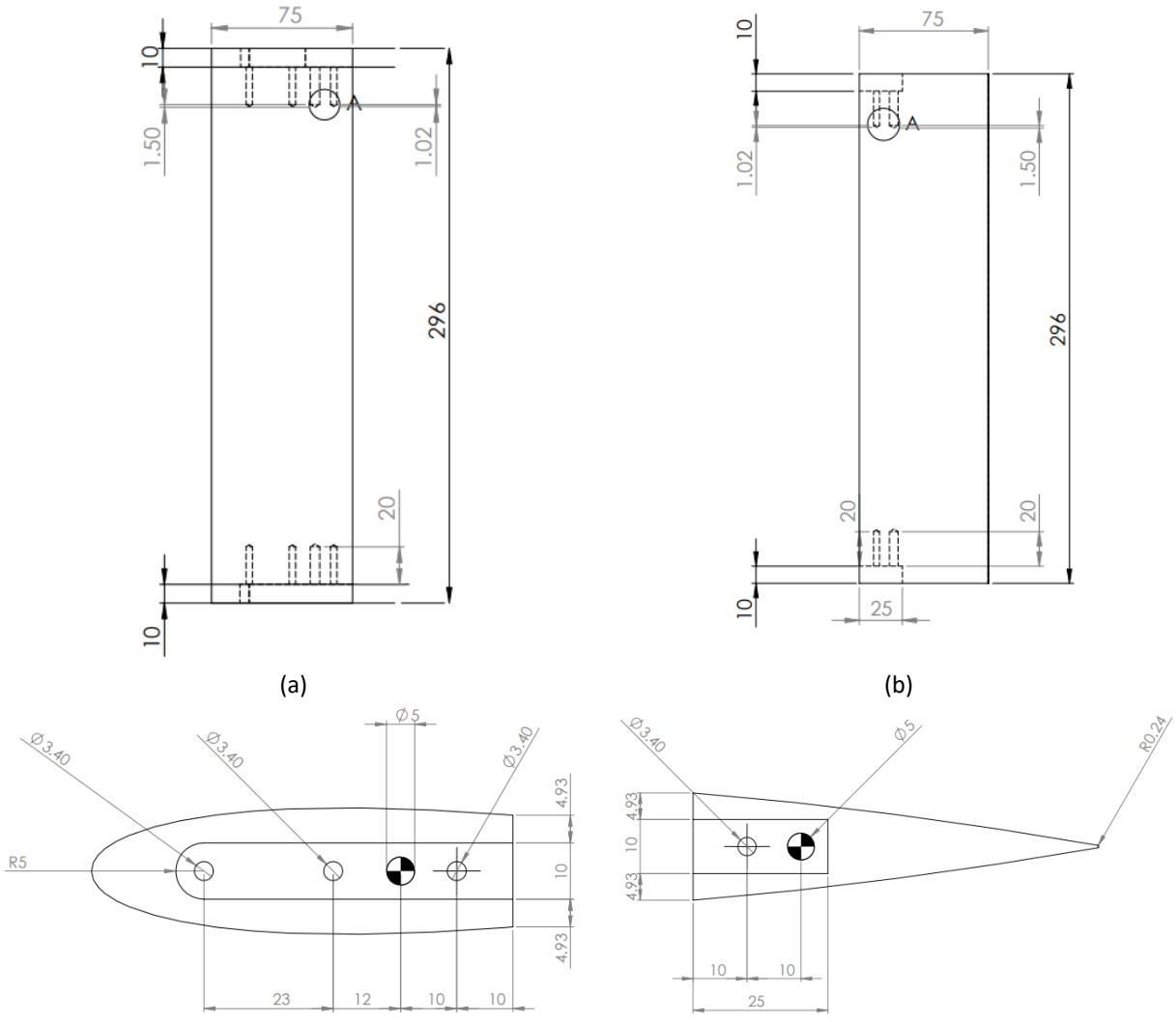

Fig. 2. Geometry of NACA0015 airfoil used in this study (a) top of the front part (b) top view of the back part (c) side view of the front part (d) side view of the back part

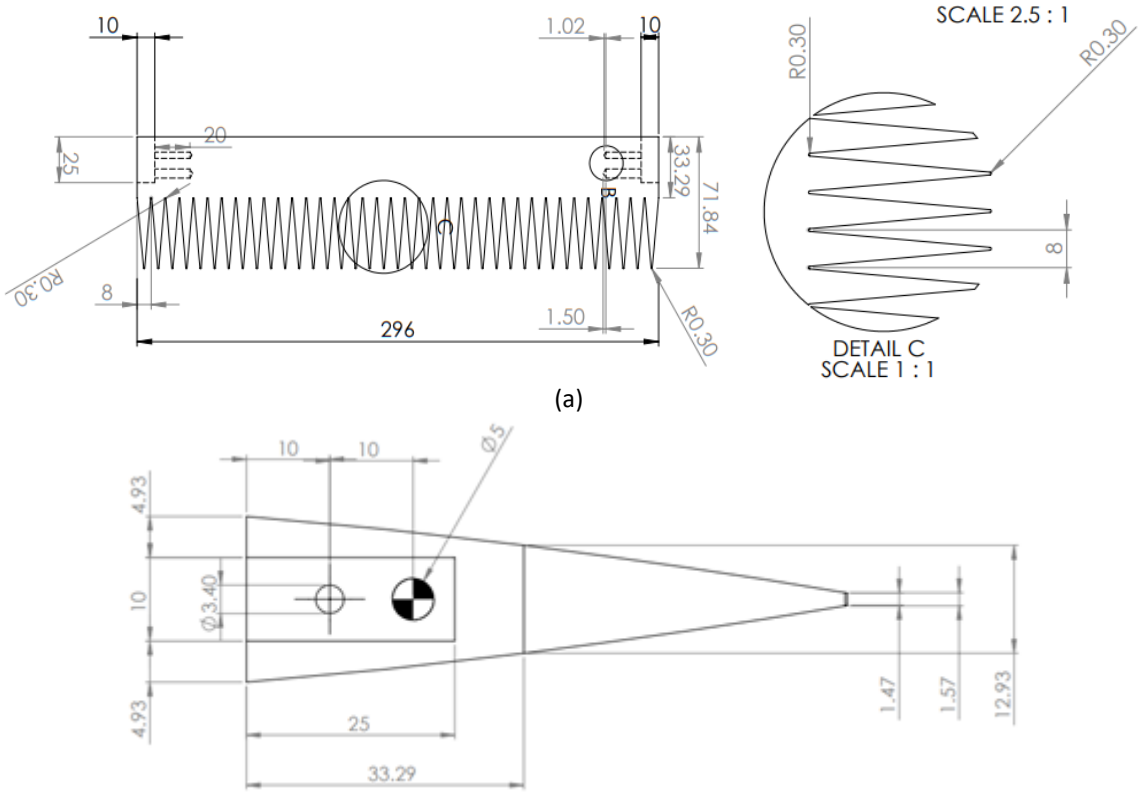

Fig. 3. Serrated trailing edge with dimensions on (a) top view and (b) side view

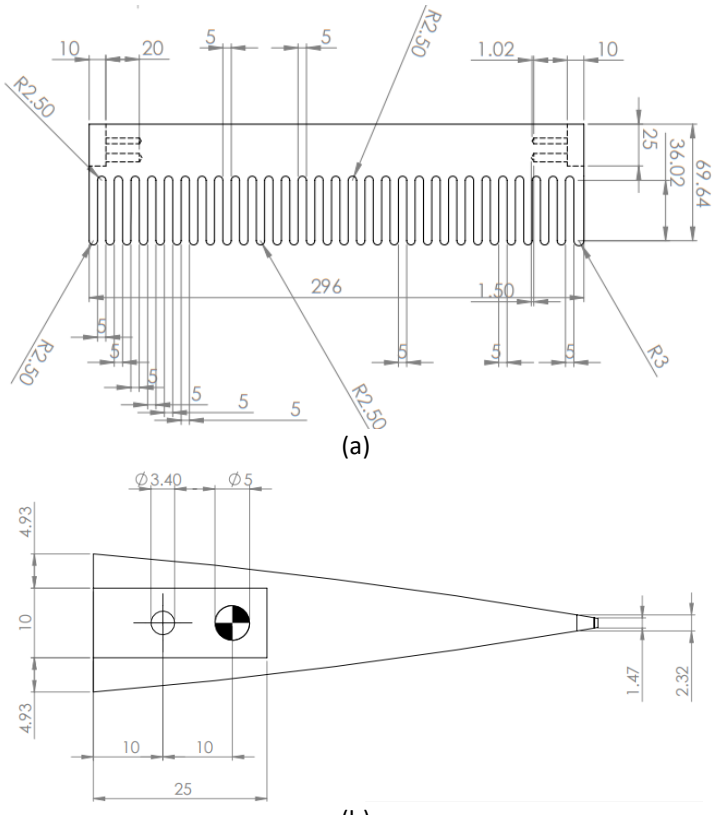

Fig. 4. Combed trailing edge with dimensions on (a) top view and (b) side view

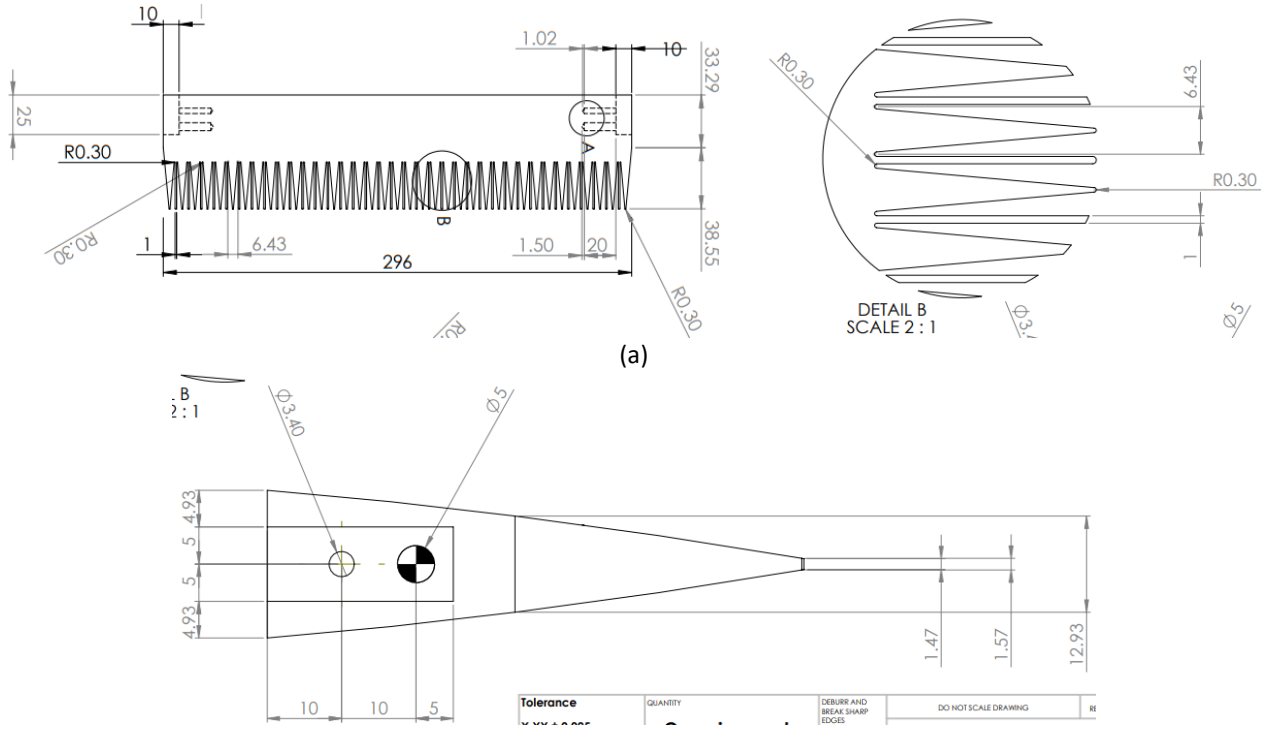

Fig. 5. Combed-serrated trailing edge with dimensions on (a) top view and (b) side view

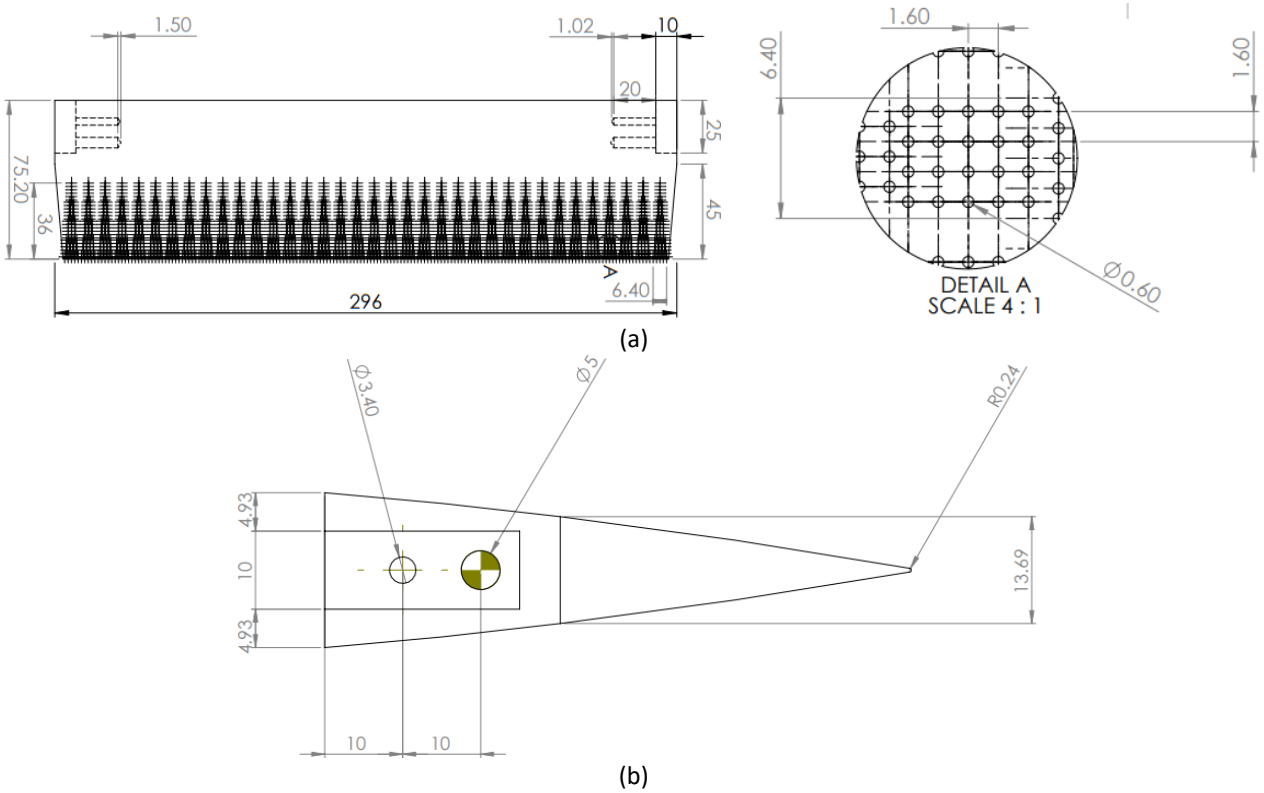

Fig. 6. Poro-serrated trailing edge with dimensions on (a) top view and (b) side view

3. Results

3.1 Validation and Comparison of Aerodynamic Parameters

The experimental investigation into the aerodynamic properties of the tested airfoil model provided significant insights, particularly concerning lift, drag, and pitching moment coefficients. The lift coefficient, a pivotal parameter governing lift generation at various angles of attack, was scrutinized as depicted in Figure 7. Analysis of the experimental data revealed a linear increase in the lift coefficient with the angle of attack until it reached a peak value. Subsequently, beyond this peak, the lift coefficient exhibited a declining trend, a behavior consistent with the characteristic lift curve of typical airfoils. Notably, the lift coefficient for Reynolds number 1.5 x 10^5 show an almost similar trend to the published and theoretical data in positive angle of attacks (3^o - 15^o), meanwhile for Reynolds number 2.0 x 10^5 shows a decrement in value as compared to published and theoretical data. Overall, the experiment yielded consistent and expected results. The lift coefficient initially increased as the angle of attack increased, reaching its maximum value at an angle of attack of around 12^o. Subsequently, a gradual decrease in the lift coefficient occurred due to flow separation. This observation is consistent with the findings found from published experimental data and Xfoil software [16]. Additionally, the measured lift coefficient closely approximated the predictions derived from thin airfoil theory before the stall angle. Beyond the stall angle, the measured lift coefficient deviates from the thin airfoil theory. This is because the thin airfoil theory was derived from incompressible and inviscid flow, which does not consider the viscous effect that leads to flow separation.

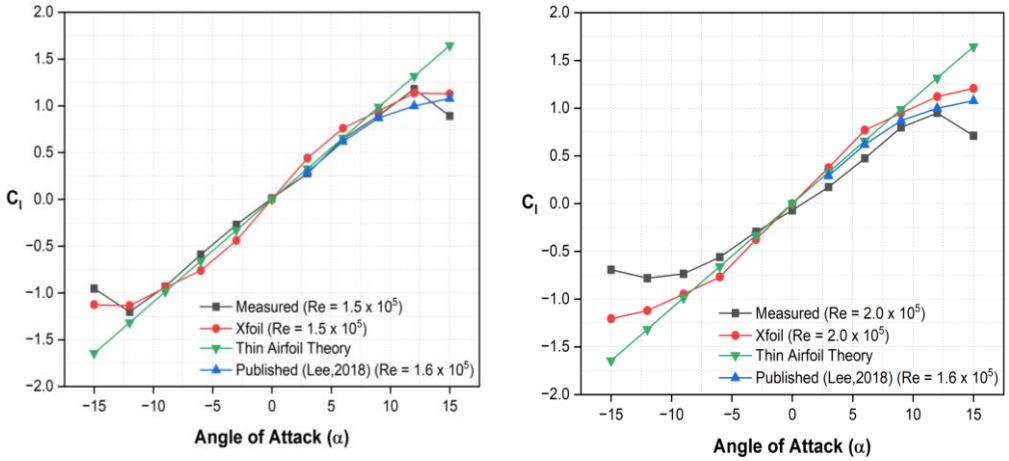

Fig. 7. Comparison of Measured, Published, and Theoretical data for lift coefficient, C_l for Baseline for different Reynolds numbers

The experimental data revealed that the drag coefficient increased almost parabolically with the angle of attack as displayed in Figure 8. This behavior is expected as the flow separation and turbulent effects increase with higher angles of attack [17]. The determined drag coefficients were consistent with published experimental data and Xfoil numerical predictions only for specific angles of attack [16]. Notably, the drag coefficient followed anticipated patterns, maintaining relatively low values at small angles of attack, indicative of laminar flow over the airfoil surface. As the angle of attack increases, the drag coefficient increases gradually due to the formation of turbulent flow and increased pressure drag [18]. However, at higher angles of attack, a significant rise in the drag coefficient was evident, suggesting flow separation and the onset of stall. In the range of negative angles of attack (-15^o - 0^o), both Reynolds numbers, 1.5 x 10^5 and 2.0 x 10^5, exhibited a gradual increase in drag compared to the theoretical data. Conversely, positive angles of attack yielded

unexpected occurrences, such as negative drag values, notably at 12^0 for 1.5×10^5. The sensor reading for the calibrated six-component balance happened to have several problems when taking the reading of drag coefficient values during the test, even though multiple measurements were taken.

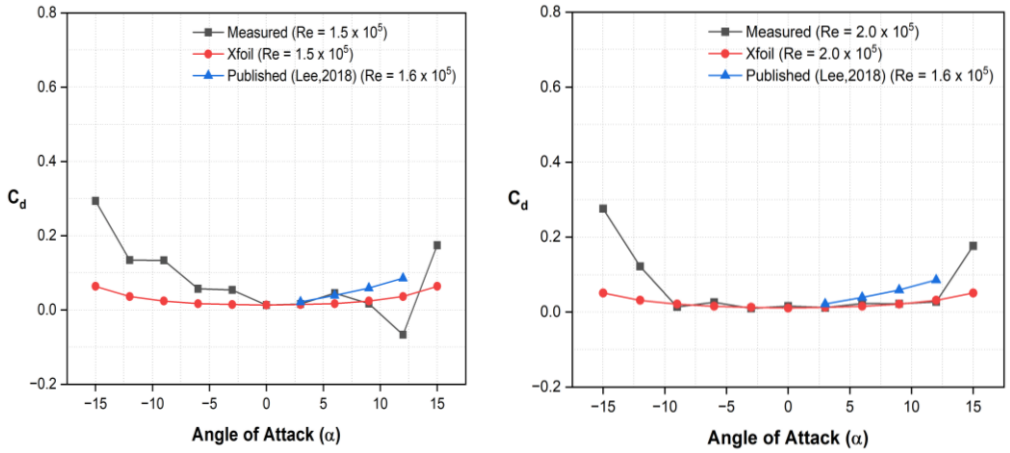

Fig. 8. Comparison of Measured, Published, and Theoretical data for drag coefficient, C_d for Baseline with different Reynolds number

The pitching moment coefficient provides insights into the static stability of the airfoil. As shown in Figure 9, the experimental measurements showed that the pitching moment coefficient initially increased with the angle of attack until reaching a peak, beyond which it decreased. This trend signifies that the airfoil experiences a shift in its center of pressure as the angle of attack changes [19].

In summary, comparing the experimental results with theoretical values and established experimental data, it was evident that the NACA 0015 airfoil exhibited typical aerodynamic characteristics [16]. The lift coefficient curve showed a well-defined peak, followed by a gradual decrease due to flow separation. The drag coefficient parabolically increases with increasing angles of attack, indicating the formation of turbulent flow and subsequent stall. Potential sources of error in the experiment could include uncertainties in the measurement equipment, inaccuracies in the angle of attack setting, and variations in the flow conditions within the wind tunnel. These factors may have contributed to slight deviations between the measured, published experimental, and theoretical results.

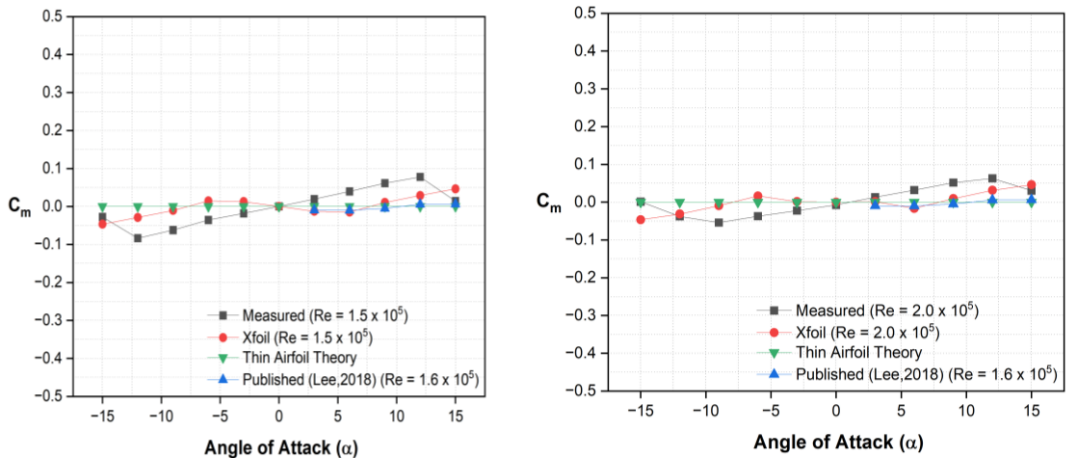

Fig. 9. Comparison of Measured, Published, and Theoretical data for moment coefficient, C_m for Baseline with different Reynolds number

3.2 Effect of Reynolds Number on the Aerodynamic Parameters of NACA 0015

This study also delved into the impact of varying Reynolds numbers on the aerodynamic characteristics of the NACA 0015 airfoil. The lift coefficient, drag coefficient, and moment coefficient were systematically measured and compared across a range of Reynolds numbers for comprehensive analysis. The lift coefficient showed a distinct increase with increasing Reynolds number as shown in Figure 10. This behavior is attributed to the improved flow attachment and reduced separation at higher Reynolds numbers [20]. The boundary layer thickness decreased, resulting in reduced viscous drag and increased lift production [21]. This trend is consistent with the theoretical expectations for laminar flow over the airfoil. It shows that for Reynolds number 1.5 x 10^5 attained greater maximum lift coefficient as compared to Reynolds number 2.0 x 10^5. At lower Reynolds numbers, the flow over the airfoil is generally more prone to separation, resulting in a lower lift coefficient. As the Reynolds number increases, the flow tends to become more attached and the boundary layer becomes thinner, reducing the effects of separation. This improved flow attachment leads to an increase in the lift coefficient. However, it is worth noting that the exact behavior of the lift coefficient concerning the Reynolds number can depend on several factors, including airfoil design, angle of attack, and flow conditions. There can be cases where the lift coefficient reaches a maximum value at a specific Reynolds number and then starts to decrease due to flow transition or other flow phenomena [22]. This behavior is typically associated with the occurrence of flow separation or stall at high Reynolds numbers.

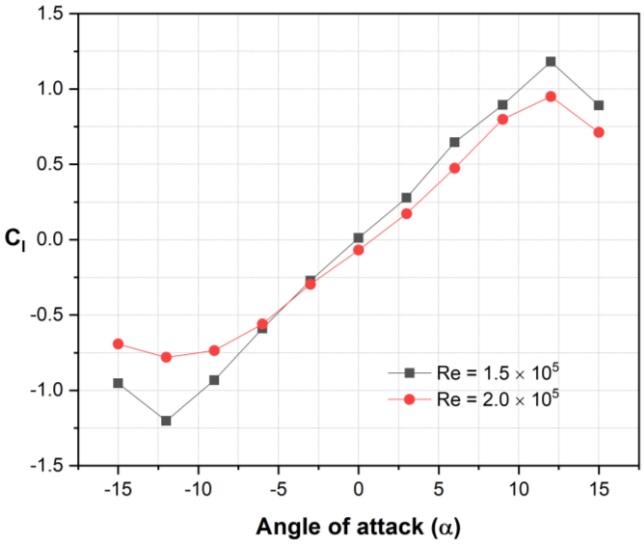

Fig. 10. Comparison of lift coefficient, C_l forbaseline with different Reynolds number

The drag coefficient decreased with increasing Reynolds number due to the reduction in skin friction drag [23]. However, as the Reynolds number continued to rise, the drag coefficient reached a minimum and started to increase. This rise in drag is primarily caused by the transition from laminar to turbulent flow, which results in increased pressure drag [24]. At high Reynolds numbers, the drag coefficient tends to plateau due to fully turbulent flow over the airfoil surface. Figure 11 below illustrates plots that exhibit consistent trends across all angles of attack. The drag coefficient generally increases with increasing angles of attack and reaches a maximum value at a certain angle of attack before potentially decreasing due to flow separation. Meanwhile, the drag coefficient is indeed higher at negative angles of attack compared to positive angles of attack. When the airfoil is subjected to a negative angle of attack (where the leading edge is facing downstream), the flow

experiences a larger pressure difference between the upper and lower surfaces of the airfoil [25]. This pressure difference contributes to an increase in the drag force acting on the airfoil. Additionally, at negative angles of attack, the airfoil may experience flow separation more readily. Flow separation occurs when the flow fails to follow the contour of the airfoil surface and detaches, leading to increased drag [26]. The flow separation at negative angles of attack can be caused by the adverse pressure gradient on the upper surface of the airfoil. At positive angles of attack, where the leading edge is facing upstream, the flow tends to remain attached to the upper surface of the airfoil for a longer distance [25]. This promotes a smoother flow and reduces the pressure difference, resulting in a lower drag force compared to negative angles of attack.

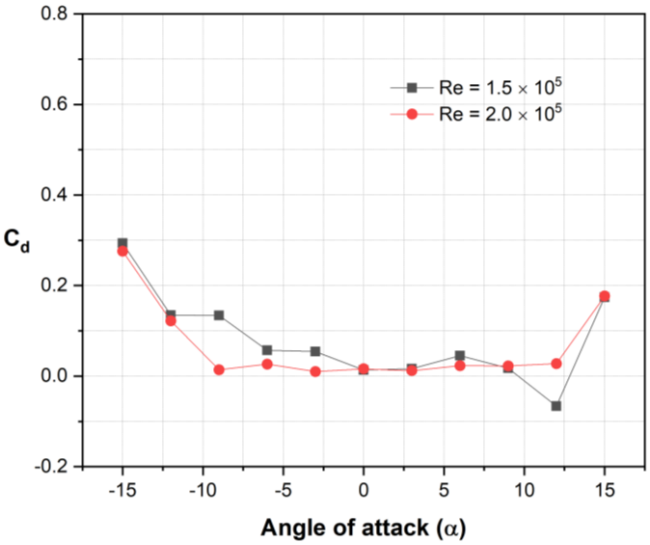

Fig. 11. Comparison of drag coefficient, C_d for Baseline with different Reynolds numbers

The moment coefficient showed a relatively small variation with the Reynolds number. However, at higher Reynolds numbers, a slight decrease in the moment coefficient was observed. This reduction can be attributed to the reduced effectiveness of the airfoil at higher Reynolds numbers, leading to a decrease in nose-down pitching moment. Figure 12 illustrates a consistent trend in the pitching moment coefficient across all angles of attack for the two Reynolds numbers under consideration. At a zero angle of attack, the distribution of the pressure forces around the airfoil tends to be symmetric, resulting in a near-zero pitching moment coefficient. However, at angles of attack significantly different from zero, the pitching moment coefficient for the airfoil may deviate from zero as changes in the angle of attack alter the pressure distribution, inducing a pitching moment that either rotates the airfoil nose-up or nose-down.

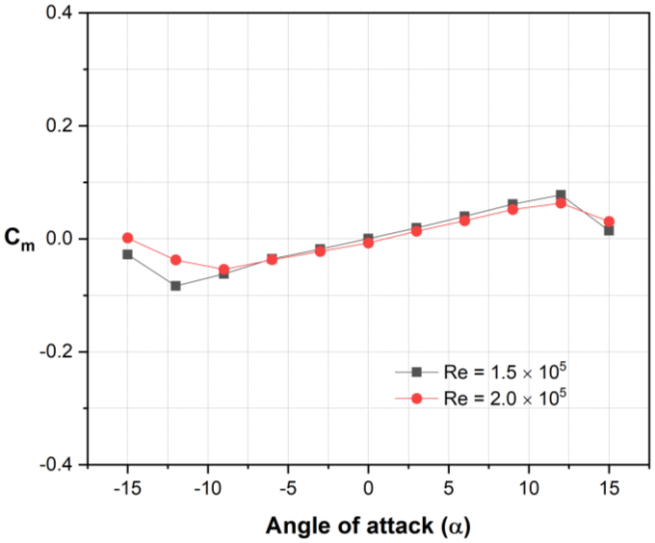

Fig. 12. Comparison of pitching moment coefficient, C_m for Baseline with different Reynolds numbers

3.3 Comparison of the Aerodynamic Parameters of NACA 0015 With Different Trailing Edges

Different types of trailing edges can have a significant impact on the aerodynamic parameters of an airfoil. In this experiment, we investigated the impact of different trailing edges, including baseline, serration, combed, comb-serration, and poro-serration, on aerodynamic parameters. The comparison of lift coefficients for these trailing edge types at various Reynolds numbers is depicted in Figure 13 below. At Reynolds numbers of 1.5 x 10^5 and 2.0 x 10^5, the lift coefficient consistently exhibits lower values across all trailing edges compared to the baseline, especially at higher angles of attack. In contrast, at lower angles of attack, the lift coefficient for both Reynolds numbers tends to follow a similar trend as the baseline. Thus, at lower angles of attack, all types of trailing edges display similar trends in the lift coefficient compared to the baseline, whereas at higher angles of attack, all types of trailing edges have the potential to degrade the lift coefficient in comparison to the baseline.

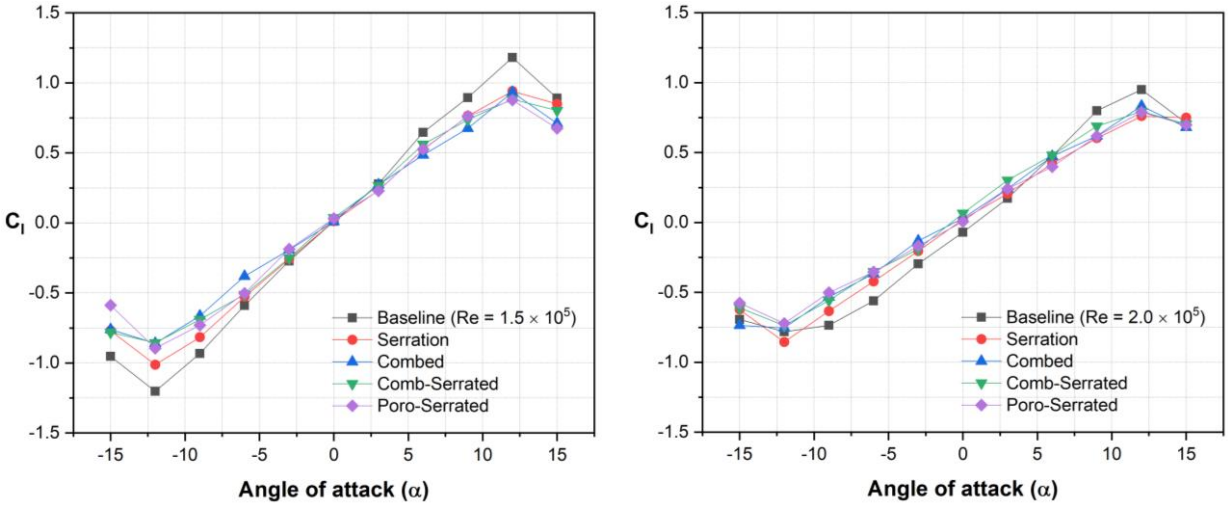

Fig. 13. Comparison of lift coefficient, C_l for Serrated with different Reynolds numbers

Figure 14 illustrates the comparison of drag coefficients for all types of trailing edges at different Reynolds numbers. For Reynolds numbers 1.5 x 10^5, most of the trailing edges exhibit higher values of drag coefficient compared to baseline up to certain angles of attack only. However, at Reynolds

number 2.0 x 10^5 the drag coefficient for all trailing edges exhibits an almost similar trend to the baseline. Hence, it can be concluded that for lower Reynolds numbers, the drag coefficients tend to be a higher value for all types of trailing edges when compared to the baseline, whereas, for higher Reynolds numbers, the drag coefficient depicts a similar trend with the baseline.

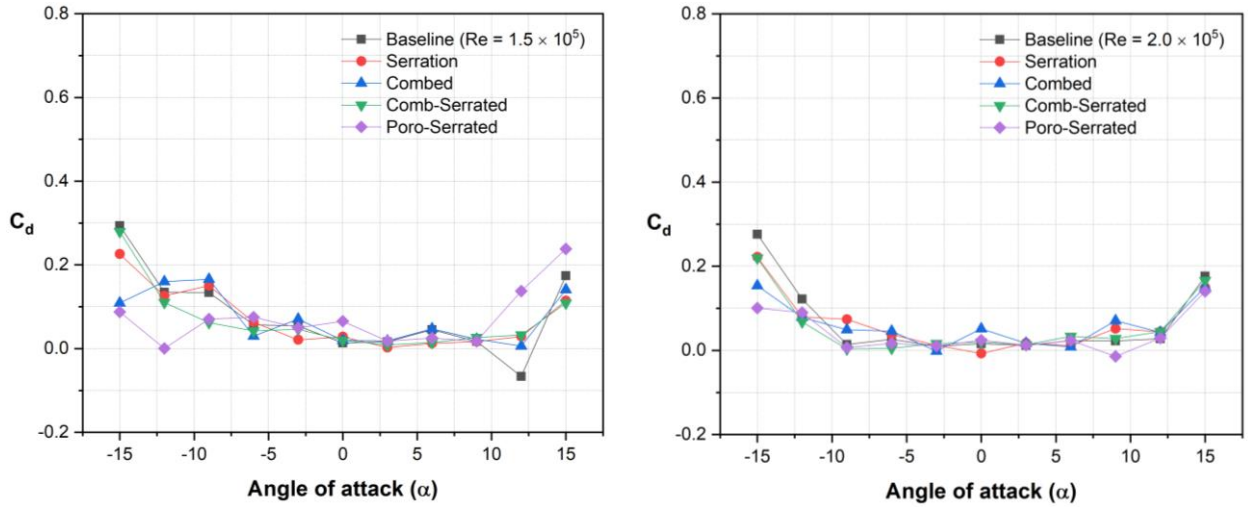

Fig. 14. Comparison of drag coefficient, C_d for Serrated with different Reynolds numbers

In Figure 15, a comprehensive analysis of the pitching moment coefficient is presented, encompassing various trailing edge configurations, including the baseline, at different Reynolds numbers. In general, all trailing edge types demonstrate similar trends to the baseline across the two Reynolds numbers. Nevertheless, slight variations in the pitching moment coefficient values emerge for these trailing edge types in comparison to the baseline, particularly at high negative angles of attack. Moreover, a slight deviation from the trend in the pitching moment coefficient values of different trailing edges compared to the baseline becomes noticeable at higher positive angles of attack.

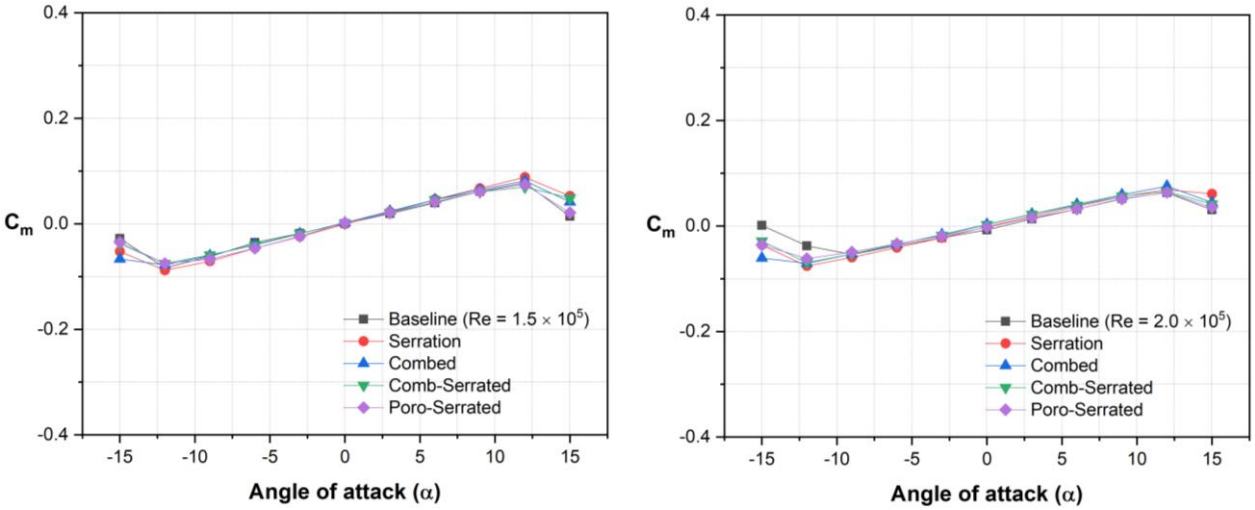

Fig. 15. Comparison of pitching moment coefficient, C_m for Serrated with different Reynolds numbers

3.4 Drag Polar Diagram

Figure 16 illustrates the lift coefficient versus drag coefficient relationship for all types of trailing edges at each different Reynolds number. It is important as it provides insights into the airfoil's performance and efficiency across different operating conditions. On top of that, results show that all types of trailing edges have the same performance for each Reynolds number, especially a Reynolds number 2.0 x 10^5, it clearly shows that all types of trailing edges have little significant effect on airfoil performance.

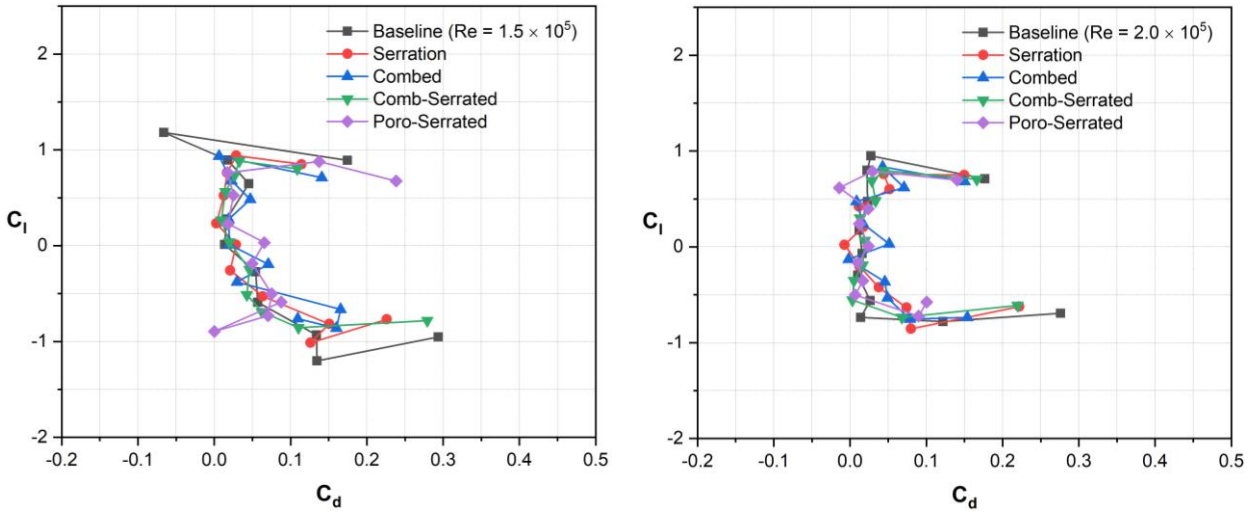

Fig. 16. Lift coefficient versus drag coefficient, $C_l \; vs \; C_d$ for all types of trailing edges at Reynolds number (a) 1.5 x 10^5 and (b) 2.0 x 10^5

4. Conclusions

In conclusion, the comprehensive analysis of various trailing edge configurations, including serration, poro-serration, comb, and comb-serration, has revealed that the airfoil with the baseline model consistently demonstrates superior aerodynamic performance. Most of the trailing edges except the baseline showed depletion in lift coefficient, c_l, showcasing its stability across a range of angles of attack. Notably, at very low angles of attack, a comparable trend in lift coefficient values is observed among the configurations. On the other hand, most of the trailing edges showed an increment in drag coefficient at Reynolds number 1.5 x 10^5. However, at Reynolds number 2.0 x 10^5, the drag coefficient exhibits an almost similar trend to the baseline. This suggests that the baseline model achieves a level of consistency in drag performance across varying Reynolds numbers. Furthermore, the analysis of pitching moment coefficient trends indicates that all types of trailing edges, in conjunction with the baseline, share a similar behavior. The comprehensive evaluation of Lift coefficient versus drag coefficient, $C_l \; vs \; C_d$ proves that, despite the variations in trailing edge configurations, their overall performance remains consistent for each Reynolds number. In essence, the baseline model emerges as the optimal choice, showcasing superior aerodynamic characteristics across the evaluated parameters.

Acknowledgment
The research was supported by the Ministry of Education (MOE) through the Fundamental Research Grant Scheme (FRGS/1/2018/TK09/UIAM/03/4). We would also like to thank the financial support of IIUM under the KOE Postgraduate Tuition Fee Waiver Scheme 2019 (TFW2019).

References

[1] Andan, Amelda Dianne, and Duck-Joo Lee. "Discrete Tonal Noise of NACA0015 Airfoil at Low Reynolds Number." *Journal of Advanced Research in Fluid Mechanics and Thermal Sciences* 53, no. 1 (2019): 129-145.

[2] Kurelek, John W., Burak A. Tuna, Serhiy Yarusevych, and Marios Kotsonis. "Three-dimensional development of coherent structures in a two-dimensional laminar separation bubble." *AIAA Journal* 59, no. 2 (2021): 493-505. https://doi.org/10.2514/1.J059700

[3] Tank, J. D., B. F. Klose, G. B. Jacobs, and G. R. Spedding. "Flow transitions on a cambered airfoil at moderate Reynolds number." *Physics of Fluids* 33, no. 9 (2021). https://doi.org/10.1063/5.0061939

[4] Nakhchi, M. E., S. Win Naung, and Mohammad Rahmati. "High-resolution direct numerical simulations of flow structure and aerodynamic performance of wind turbine airfoil at wide range of Reynolds numbers." *Energy* 225 (2021): 120261. https://doi.org/10.1016/j.energy.2021.120261

[5] Kurelek, John. "Transition in a Laminar separation bubble and the effect of acoustic excitation." *Master's thesis, University of Waterloo*, 2016.

[6] Souppez, Jean-Baptiste R. G., Patrick Bot, and Ignazio Maria Viola. "On the Effect of the Leading-Edge Separation Bubble on the Aerodynamics of Spinnakers." In *7th High Performance Yacht Design Conference*, pp. 1-11. RINA NZ, 2022.

[7] Ibren, Mohamed, Amelda Dianne Andan, Waqar Asrar, and Erwin Sulaeman. "Laminar Separation Bubble and Flow Topology of NACA 0015 at Low Reynolds Number." *CFD Letters* 13, no. 10 (2021): 36-51. https://doi.org/10.37934/cfdl.13.10.3651

[8] Rubel, Robiul Islam, Md Kamal Uddin, Md Zahidul Islam, and M. D. Rokunuzzaman. "Numerical and experimental investigation of aerodynamics characteristics of NACA 0015 aerofoil." *International Journal of Engineering Technologies IJET* 2, no. 4 (2016): 132-141. https://doi.org/10.19072/ijet.280499

[9] Aldheeb, Mohammed, Waqar Asrar, Erwin Sulaeman, and Ashraf A. Omar. "Aerodynamics of porous airfoils and wings." *Acta Mechanica* 229 (2018): 3915-3933. https://doi.org/10.1007/s00707-018-2203-6

[10] Vathylakis, Alexandros, Tze Pei Chong, and Phillip F. Joseph. "Poro-serrated trailing-edge devices for airfoil self-noise reduction." *AIAA Journal* 53, no. 11 (2015): 3379-3394. https://doi.org/10.2514/1.J053983

[11] Ethiraj, Livya, and Subramania Nadaraja Pillai. "Effect of trailing-edge modification over aerodynamic characteristics of NACA 0020 airfoil." *Wind and Structures* 33, no. 6 (2021): 463-470.

[12] Ebrahimi, Abbas, Majid Hajipour, and Kamran Ghamkhar. "Experimental study of stall control over an airfoil with dual excitation of separated shear layers." *Aerospace Science and Technology* 82 (2018): 402-411. https://doi.org/10.1016/j.ast.2018.09.027

[13] Xu, He-Yong, Qing-Li Dong, Chen-Liang Qiao, and Zheng-Yin Ye. "Flow control over the blunt trailing edge of wind turbine airfoils using circulation control." *Energies* 11, no. 3 (2018): 619. https://doi.org/10.3390/en11030619

[14] Menon, Muraleekrishnan, Fernando Ponta, Xiao Sun, and Qingli Dai. "Aerodynamic analysis of flow-control devices for wind turbine applications based on the trailing-edge slotted-flap concept." *Journal of Aerospace Engineering* 29, no. 5 (2016): 04016037. https://doi.org/10.1061/(ASCE)AS.1943-5525.0000623

[15] Gall, Peter D. *A numerical and experimental study of the effects of dynamic roughness on laminar leading edge separation*. West Virginia University, 2010.

[16] Lee, T., and V. Tremblay-Dionne. "Experimental investigation of the aerodynamics and flowfield of a NACA 0015 airfoil over a wavy ground." *Journal of Fluids Engineering* 140, no. 7 (2018): 071202. https://doi.org/10.1115/1.4039236

[17] Roy, Aritras, Arnab Kumar Mallik, and Tushar Pratim Sarma. "A Study of Model Separation Flow Behavior at High Angles of Attack Aerodynamics." *Journal of Applied and Computational Mechanics* 4, no. 4 (2018): 318-330.

[18] Eftekhari, Shahrooz, and Abdulkareem Shafiq Mahdi Al-Obaidi. "Investigation of a NACA0012 finite wing aerodynamics at low Reynold's numbers and 0º to 90º angle of attack." *Journal of Aerospace Technology and Management* 11 (2019): e1519. https://doi.org/10.5028/jatm.v11.1023

[19] Maji, Arnesh, Jawahar Sivabharathy Samuthira Pandi, and Sanjay Mittal. "Aerodynamic center of a Finite Wing at low Reynolds Number." *Korean Society of Computational Fluid Engineering* (2022): 89-90.

[20] Brunner, Claudia E., Janik Kiefer, Martin OL Hansen, and Marcus Hultmark. "Study of Reynolds number effects on the aerodynamics of a moderately thick airfoil using a high-pressure wind tunnel." *Experiments in Fluids* 62 (2021): 1-17. https://doi.org/10.1007/s00348-021-03267-8

[21] Lyu, Yu Zhu, Hao Jie Zhu, and Mao Sun. "Aerodynamic forces and vortical structures of a flapping wing at very low Reynolds numbers." *Physics of Fluids* 31, no. 4 (2019). https://doi.org/10.1063/1.5089804

[22] Li, Zhenyao, Lihao Feng, Hamid Reza Karbasian, Jinjun Wang, and Kyung Chun Kim. "Experimental and numerical investigation of three-dimensional vortex structures of a pitching airfoil at a transitional Reynolds number." *Chinese Journal of Aeronautics* 32, no. 10 (2019): 2254-2266. https://doi.org/10.1016/j.cja.2019.04.015

[23] Raayai-Ardakani, Shabnam, and Gareth H. McKinley. "Drag reduction using wrinkled surfaces in high Reynolds number laminar boundary layer flows." *Physics of Fluids* 29, no. 9 (2017). https://doi.org/10.1063/1.4995566

[24] Nick, Nathalie, and Yohei Sato. "Computational fluid dynamics simulation of Hyperloop pod predicting laminar-turbulent transition." *Railway Engineering Science* 28 (2020): 97-111. https://doi.org/10.1007/s40534-020-00204-z

[25] Livya, E., and S. Nadaraja Pillai. "Effect of turbulence intensity on aerodynamic characteristics of extended trailing edge airfoil." *Aircraft Engineering and Aerospace Technology* 94, no. 10 (2022): 1780-1791. https://doi.org/10.1108/AEAT-12-2021-0382

[26] Sadikin, Azmahani, Nurul Akma Mohd Yunus, Saiful Anuar Abd Hamid, Salihatun Md Salleh, Mohd Nasrull Abdol Rahman, Shahruddin Mahzan, and Sallehuddin Shah Ayop. "A comparative study of turbulence models on aerodynamics characteristics of a NACA0012 airfoil." *International Journal of Integrated Engineering* 10, no. 1 (2018).